

Efficient Multi-Task and Multi-Robot Transfer with Continued Learning

Karime Pereida, Mohamed K. Helwa and Angela P. Schoellig

Abstract—Ideally, robots should learn from a few demonstrations of a given task, and generalize knowledge to new, unseen tasks, and to different robots. In this paper, we focus on trajectory tracking and introduce a multi-robot, multi-task transfer learning framework that allows a target system to complete a target task by learning from a few demonstrations of a source task on a source system. The proposed *multi-robot* transfer learning framework is based on a combined \mathcal{L}_1 adaptive control and iterative learning control approach. The key idea is that the adaptive controller forces dynamically different systems to behave as the specified reference model. The proposed *multi-task* transfer learning framework uses theoretical control results (e.g. the concept of vector relative degree) to learn a map from desired trajectories to the inputs that make the system track these trajectories. The learned map is then used to calculate the inputs for a new, unseen trajectory. Experimental results using two different quadrotors show that, using the proposed framework, it is possible to significantly reduce the tracking error of a target trajectory on the target system when information from a single source trajectory learned on the source system is used.

I. INTRODUCTION

We are interested in designing learning-based control methods that allow robots and automated systems to perform a variety of complex tasks in changing environments. To guarantee high overall performance in these environments, the proposed control methods must be able to handle model uncertainties, unknown disturbances and changing dynamics. The learning controller must be robust to changes in the environmental conditions. This is in contrast to traditional, model-based controllers, where small changes in the conditions may significantly deteriorate the controller performance and may cause instability (see [1], [2] and [3]). Learning-based controllers aim to handle uncertain and changing dynamics without the need for knowing the exact model.

Training robots to operate in changing environments is complex and time-consuming; hence, in this paper we develop a framework that allows robots to learn from few demonstrations of a given task, and generalize this knowledge to new tasks (multi-task framework) and to new robots (multi-robot framework), without requiring hand-tuning or experimental trial-and-error, see Fig. 1. We focus on trajectory tracking as many robotic tasks can be described as trajectory tracking problems, for example, in application areas such as manufacturing, rehabilitation, and unmanned aerial vehicle (UAV) stage entertainment. Moreover, for some

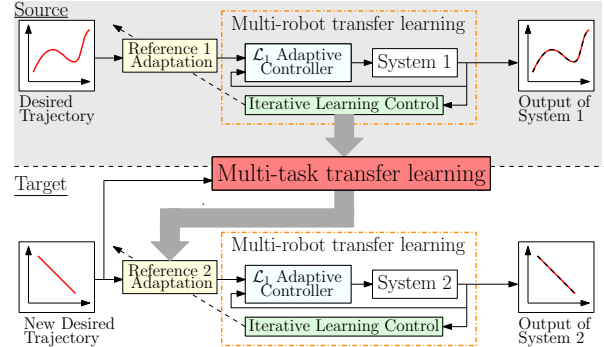


Fig. 1. The proposed multi-robot, multi-task architecture. The multi-robot transfer learning framework is composed of two methods (i) an iterative learning control (ILC) module to learn an input such that the output tracks a desired output signal and (ii) an \mathcal{L}_1 adaptive controller to force different systems to behave in the same repeatable, predefined way. Hence, trajectories learned on a source system can directly be transferred to a target system. The multi-task transfer learning framework learns a map from a desired trajectory to the inputs that make the system track it accurately. When a new trajectory is encountered, the learned map is used to calculate the inputs for the new trajectory.

applications, it is advantageous, given time, safety and budget considerations, to use a different robot hardware for the initial control design and training, rather than the hardware used for the actual, final task execution. Multi-robot transfer learning saves the time needed for training each new robot and reduces the unavoidable risks of the training phase. In this work, we present a multi-task, multi-robot transfer framework that guarantees high performance across a wide range of robot dynamics and tasks.

Little work is available on strategies for multi-robot transfer learning. In [4], a simplified transfer learning scenario for two linear, time-invariant (LTI), single-input, single-output (SISO) systems is analyzed. In this scenario, the two systems are tasked to follow the same learning reference, and an optimal static gain is learned between the outputs of the two systems. The analysis shows that the transformation error is minimized when the two systems have stable poles that lie close to each other. The extension in [5] shows a preliminary study of transfer learning between two nonlinear, unicycle robots. In [6], it is proved that the optimal transfer learning map between two robots is, in general, a dynamic system. Moreover, [6] provides an algorithm for determining the properties of the optimal dynamic map, including its order, relative degree and the variables it depends on, from easy-to-execute experiments. In [7], a data transfer mechanism based on manifold alignment of input-output data is proposed. The transferred data improves learning of a model of a robotic arm by using data from a different robotic arm.

The field of multi-task transfer has been studied more

The authors are with the Dynamic Systems Lab (www.dynsyslab.org) at the University of Toronto Institute for Aerospace Studies (UTIAS), Canada. Email: k.pereidaperez@mail.utoronto.ca, mohamed.helwa@robotics.utias.utoronto.ca, schoellig@utias.utoronto.ca

This research was supported in part by the Mexican National Council of Science and Technology (abbreviated CONACYT).

extensively and multiple different approaches have been proposed [8]–[11]. Learning approaches, such as iterative learning control (ILC), usually have the limitation of not being able to generalize or transfer knowledge from previously learned tasks to new, unseen tasks. In [8], using knowledge from previously learned trajectories, a linear map is created to improve the initialization of the inputs required to track unseen trajectories. Experimental results show that only one learned trajectory is needed for improving performance on a new trajectory. However, the choice of the variables necessary for creating the linear map is based on experiments, which may require a lot of experimental runs. Moreover, [8] does not present multi-robot transfer. In [9] and [10], a deep neural network (DNN) is trained to achieve a unity map between the desired and actual outputs. In particular, the DNN adapts the reference signal to a feedback control loop to enhance the tracking performance of unseen trajectories. In [12], neural networks allow generalization of a task, such as block stacking, based on a single instance of the given task, such as a different block stacking configuration. However, the architecture of the neural network has to be tailored for the specific task.

In the realm of multi-task and multi-robot transfer, the work in [13] trains neural network policies that can be decomposed into “task-specific” and “robot-specific” modules. Task-specific modules are shared across robots, and robot-specific modules are shared across all tasks on that robot. When a new robot-task combination is encountered, the appropriate robot and task modules can be composed to solve the problem. This architecture enables zero-shot generalization with a variety of robots and tasks in simulation. Neural network approaches require a significant amount of data and computational resources to train. In this paper, we focus on using as few demonstrations as possible to achieve successful transfer in experiments.

The goal of this work is to design a learning architecture that is able to achieve high-accuracy tracking (i) despite the presence of unmodeled disturbances and changing dynamics caused by the environment or by switching the robot hardware altogether, and (ii) by using previously learned trajectories and generalizing knowledge to new, unseen trajectories. We propose a multi-task framework on top of a multi-robot transfer learning framework (see Fig. 1). The proposed multi-task learning scheme does not require exact knowledge of the system model or significant amounts of data as in [13].

The multi-robot transfer framework is based on the combined \mathcal{L}_1 adaptive control and ILC framework proposed in [14]. The \mathcal{L}_1 adaptive controller forces dynamically-different systems to behave as a specified reference model. The ILC improves tracking performance over iterations. Hence, learned trajectories on the source system can be transferred among dynamically different target systems (equipped with the same underlying \mathcal{L}_1 adaptive controller) to achieve high-accuracy tracking. The multi-task framework learns a map between a single desired trajectory and the inputs that make the system track the desired trajectory accurately. This map is then used to calculate the inputs needed to perfectly track a

new, unseen trajectory. Unlike [8], which used experimental trial-and-error, we derive this map based on concepts from control theory, particularly the concept of vector relative degree. The proposed approach also allows the target system to keep learning over iterations to further improve its tracking performance.

The remainder of this paper is organized as follows. The problem is defined in Section III. The details of the proposed approach and the main results are presented in Section IV. Experimental results on two quadrotors are presented in Section V. Conclusions are provided in Section VI.

II. BACKGROUND

In this section, we review the definitions needed for the remainder of the paper. Consider a discrete-time, linear time-invariant (LTI), multi-input, multi-output (MIMO) system:

$$\begin{aligned} x(k+1) &= Ax(k) + Bu(k) \\ y(k) &= Cx(k), \end{aligned} \quad (1)$$

where $x(k) \in \mathbb{R}^n$ is the system state vector, $u(k) = [u_1(k), \dots, u_p(k)]^T \in \mathbb{R}^p$ is the system input, $y(k) = [y_1(k), \dots, y_p(k)]^T \in \mathbb{R}^p$ is the system output, k is the discrete-time index, and B and C are full rank. Let

$$B = [B_1, \dots, B_p] \quad \text{and} \quad C = [C_1^T, \dots, C_p^T]^T.$$

Definition 1 (Vector relative degree). System (1) is said to have a vector relative degree (r_1, \dots, r_p) if

- (i) $C_i A^k B_j = 0, \forall i = \{1, \dots, p\}, \forall j = \{1, \dots, p\}$ and $\forall k = \{0, \dots, r_i - 2\}$,
- (ii) and the decoupling matrix A_0 where $[A_0]_{ij} = C_i A^{r_i - 1} B_j, \forall i, j \in \{1, \dots, p\}$ is nonsingular.

Remark 1. If the system (1) has a vector relative degree (r_1, \dots, r_p) , then we have

$$\begin{bmatrix} y_1(k+r_1) \\ \vdots \\ y_p(k+r_p) \end{bmatrix} = \begin{bmatrix} C_1 A^{r_1} \\ \vdots \\ C_p A^{r_p} \end{bmatrix} x(k) + A_0 \begin{bmatrix} u_1(k) \\ \vdots \\ u_p(k) \end{bmatrix}. \quad (2)$$

For single-input single-output (SISO) systems, the relative degree is the number of sample delays between changing the input and observing a change of the output, and can be easily determined experimentally from the system’s step response.

Remark 2. Analogous to the case of SISO systems, the vector relative degree of a MIMO system can be determined from easy-to-execute experiments. In particular, one can carry out p experiments; in each experiment, one should apply a unit step input to only one of the p inputs, and monitor the responses of the p outputs. From Definition 1 a good estimate of the relative degree r_i is the number of sample delays between changing any of the inputs and seeing a change in the output y_i .

In other words, for the p easy-to-execute experiments, one can observe the minimum time delay obtained from the different experiments for each output dimension. After estimating the vector relative degree (r_1, \dots, r_p) , one still needs to verify that A_0 is invertible, see Definition 1. Note that from Remark 1, the rank of A_0 can be indirectly checked by studying the rank of Y_r where $[Y_r]_{ij} = y_i(r_i)|_j$ and $y_i(r_i)|_j$ is the value of the output y_i at time index r_i for the step input experiment j , and assuming that for the p experiments, the step inputs are applied at time index 0 and the system is initiated from the same initial condition x_0 .

We next review the definition of zero dynamics. The *zero dynamics* of (1) are the invariant dynamics under which the system (1) evolves when the output y is constrained to be zero for all times. The zero dynamics represent the internal dynamics of the system when the system output is stabilized to zero. By representing the system (1) in the so-called Byrnes-Isidori normal form, it can be shown that the order of the minimum realization of the zero dynamics is $n-r$, where $r = \sum_{i=1}^p r_i$ [15], [16]. The system (1) is *minimum phase* if its zero dynamics are asymptotically stable in the Lyapunov sense. Based on the definition of zero dynamics and from (2), it can be shown that if the system (1) is minimum phase, then the input $u(k) = -A_0^{-1}[(C_1 A^{r_1})^T, \dots, (C_p A^{r_p})^T]^T x(k)$ achieves asymptotic stability of the internal dynamics of (1). We use this fact in Section IV-B.

Finally, we review the definition of the projection operator, which will be used in Section IV-A. We define ∇ as the vector differential operator.

Definition 2 (Projection operator). Consider a convex compact set with a smooth boundary given by $\Omega_c := \{\lambda \in \mathbb{R}^n | f(\lambda) \leq c\}$, $0 \leq c \leq 1$, where $f : \mathbb{R}^n \rightarrow \mathbb{R}$ is the following smooth convex function:

$$f(\lambda) := \frac{(\epsilon_\lambda + 1)\lambda^T \lambda - \lambda_{max}^2}{\epsilon_\lambda \lambda_{max}^2}$$

with λ_{max} being the norm bound imposed on the vector λ , and $\epsilon_\lambda > 0$ is the projection tolerance bound of our choice. The projection operator is defined as:

$$\text{Proj}(\lambda, y) := \begin{cases} y & \text{if } f(\lambda) < 0 \\ y & \text{if } f(\lambda) \geq 0 \text{ and } \nabla f^T y \leq 0 \\ y - f_\lambda & \text{if } f(\lambda) \geq 0 \text{ and } \nabla f^T y > 0 \end{cases}$$

where $f_\lambda = \frac{\nabla f \nabla f^T y}{\|\nabla f\|^2} f(\lambda)$.

III. PROBLEM STATEMENT

The objective of this work is to achieve high-accuracy trajectory tracking in a multi-robot, multi-task framework, in which (i) there are uncertain, possibly changing environmental conditions, (ii) the training and testing robots are dynamically different, and (iii) the training and testing tasks are different. We consider a control architecture as shown in Fig. 1. A multi-task framework is added on top of a multi-robot framework.

The multi-robot framework combines an adaptive controller with a learning-based controller as in [14]. The adap-

tive controller forces two dynamically-different, minimum-phase systems to behave in the same predefined way, as specified by a reference model. The learning-based controller improves the tracking performance over iterations. Since dynamically different systems are forced to behave in the same predefined way, trajectories learned on a training system can be directly applied to a different testing system achieving high trajectory tracking performance.

In the multi-task framework, information of the desired trajectory and the learned input trajectory $(y_2^{*,l}, u_2^l)$ for a single, previously learned trajectory l is given where the subscript 2 is used to agree with the multi-robot framework notation. We aim to determine a map \mathcal{M} from the desired outputs $y_2^{*,l}$ to the learned inputs u_2^l , such that the error between $\mathcal{M}y_2^{*,l}$ and u_2^l is minimized, i.e., we need to solve

$$\min_{\mathcal{M}} \|\mathcal{M}y_2^{*,l} - u_2^l\|. \quad (3)$$

We show in this paper that for linearized or LTI systems the map \mathcal{M} is time- and state-invariant, and consequently, when a new desired trajectory $l+1$ is encountered, an input trajectory that minimizes the trajectory tracking error can be calculated by:

$$u_2^{l+1} = \mathcal{M}y_2^{*,l+1}. \quad (4)$$

Unlike [8] where the structure of the map \mathcal{M} is calculated from experimental trial-and-error, we use results from control systems theory to provide design guidelines for calculating the map \mathcal{M} .

IV. METHODOLOGY

In this section, we describe in detail the multi-robot and multi-task transfer architectures for MIMO systems.

A. Multi-robot transfer

In this work we focus on MIMO systems. Therefore, any **MIMO \mathcal{L}_1 adaptive controller** implementation, such as [17], [18], can be used. For convenience and completeness, we present the MIMO \mathcal{L}_1 adaptive controller that we implemented in our experiments in Section V. The extended \mathcal{L}_1 adaptive controller assumes that the uncertain and changing dynamics of the robotic system can be described by a MIMO system for output feedback:

$$y_1(s) = A(s)(u_{\mathcal{L}_1}(s) + d_{\mathcal{L}_1}(s)), \quad y_2(s) = \frac{1}{s}y_1(s) \quad (5)$$

where $y_1(s)$ and $y_2(s)$ are the Laplace transforms of the translational velocity $y_1(t) \in \mathbb{R}^p$ and the position $y_2(t) \in \mathbb{R}^p$, respectively, $A(s)$ is a transfer function matrix of strictly-proper *unknown* transfer functions that can be stabilized by a proportional-integral controller, $u_{\mathcal{L}_1}(s)$ is the Laplace transform of the input $u_{\mathcal{L}_1}(t) \in \mathbb{R}^p$, and $d_{\mathcal{L}_1}(s)$ is the Laplace transform of disturbance signals defined as: $d_{\mathcal{L}_1}(t) := f(t, y_1(t))$, where $f : \mathbb{R} \times \mathbb{R}^p \rightarrow \mathbb{R}^p$ is an *unknown* map subject to the global Lipschitz continuity assumption with Lipschitz constant L (see Assumption 4.1.1 in [19]).

The \mathcal{L}_1 adaptive output feedback controller aims to design a control input $u_{\mathcal{L}_1}(t)$ such that the output $y_2(t) \in \mathbb{R}^p$ tracks a bounded piecewise continuous reference input $u_2(t) \in \mathbb{R}^p$.

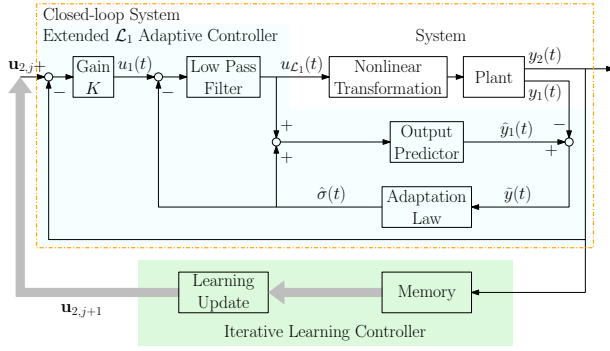


Fig. 2. The multi-robot transfer learning architecture combining the extended \mathcal{L}_1 adaptive control and the iterative learning control. Figure adopted from [14]

As illustrated in Fig. 2, we aim to achieve a desired closed-loop behavior by nesting the output of the \mathcal{L}_1 adaptive controller with output $y_1(t) \in \mathbb{R}^p$ which tracks $u_1(t) \in \mathbb{R}^p$ within a proportional feedback loop. The desired inner loop behavior is given by the following first-order reference dynamic systems:

$$M(s) = \text{diag}(M_1(s), \dots, M_p(s)), \quad M_i(s) = \frac{m_i}{s + m_i}, \quad (6)$$

where $m_i > 0$. We can rewrite the system (5) in terms of the reference system (6) as follows:

$$y_1(s) = M(s)(u_{\mathcal{L}_1}(s) + \sigma(s)), \quad y_2(s) = \frac{1}{s}y_1(s), \quad (7)$$

where the uncertainties in $A(s)$ and $d_{\mathcal{L}_1}(s)$ are combined into $\sigma(s)$ (see [14] for further details on $\sigma(s)$). The equations that describe the implementation of the extended \mathcal{L}_1 output feedback controller are presented below:

Output Predictor: $\hat{y}_1(s) = M(s)(u_{\mathcal{L}_1}(s) + \hat{\sigma}(s))$, where $\hat{\sigma}(s)$ is the adaptive estimate of $\sigma(s)$.

Adaptation Law: $\hat{\sigma}(t) = \Gamma \text{Proj}(\hat{\sigma}(t), -\hat{y}(t))$, with $\hat{\sigma}(0) = 0$, where $\hat{y}(t) := \hat{y}_1(t) - y_1(t)$ and $\text{Proj}(\cdot, \cdot)$ is defined in Section II. The adaptation rate $\Gamma > 0$ is subject to the lower bound specified in [19] and is set very large for fast adaptation.

Control Law: $u_{\mathcal{L}_1}(s) = V(s)(u_1(s) - \hat{\sigma}(s))$, where $V(s)$ is a diagonal transfer function matrix of low-pass filters:

$$V(s) = \text{diag}(V_1(s), \dots, V_p(s)), \quad V_i(s) = \frac{\omega_i}{s + \omega_i},$$

where $\omega_i > 0$. By filtering out the high frequencies in $\hat{\sigma}(s)$, high adaptation gains can be used without deteriorating the transient behavior of the system.

Closed-Loop Feedback:

$$u_1(s) = K(u_2(s) - y_2(s)), \quad (8)$$

where $K = \text{diag}(K_1, \dots, K_p)$, and $K_i \in \mathbb{R}^+$ is a proportional gain. Used to make $y_2(t)$ track $u_2(t)$.

We design $V(s)$, K , and $M(s)$ such that $H(s) = A(s)(I - V(s) + V(s)M^{-1}(s)A(s))^{-1}$ and $F(s) = (sI + H(s)V(s)K)^{-1}$ are stable, and the following \mathcal{L}_1 -norm condition is satisfied $\|F(s)H(s)(1 - V(s))\|_{\mathcal{L}_1} < 1$, where L

is the global Lipschitz constant on the disturbance function f (see Assumption 4.1.1 in [19]).

The extended \mathcal{L}_1 adaptive controller makes the system (roughly) behave as a linear, MIMO system described by:

$$y_2(s) = \text{diag}(D_1(s), \dots, D_p(s))u_2(s), \quad \text{where} \quad (9)$$

$$D_i(s) = \frac{K_i m_i}{s^2 + m_i s + K_i m_i}.$$

We use an **optimization-based ILC** [20] to improve the tracking performance of the system, which now behaves close to (9), in a small number of iterations $1, \dots, j$. The objective is to make $y_2(t)$ track a desired output trajectory $y_2^*(t)$, which is defined over a finite-time interval. We assume that there exist input, state and output trajectories $(u_2^*(t), x^*(t), y_2^*(t))$ that are feasible with respect to the true dynamics of the \mathcal{L}_1 -controlled system under linear constraints on the system inputs and/or outputs. We also assume that the system stays close to the desired trajectory; hence, we only consider small deviations from the above trajectories $(\tilde{u}_2(t), \tilde{x}(t), \tilde{y}_2(t))$. The small deviation signals are discretized since the input of computer-controlled systems is sampled and measurements are only available at fixed time intervals. The output and input trajectories can be written in the lifted representation, see [21], as $\tilde{y}_2 = [\tilde{y}_2^T(1), \dots, \tilde{y}_2^T(N)]^T$, where $N < \infty$ is the number of discrete samples, $\tilde{y}_2(k) = [\tilde{y}_{2,1}(k), \dots, \tilde{y}_{2,p}(k)]^T \in \mathbb{R}^p$ and $\tilde{u}_2 = [\tilde{u}_2^T(0), \dots, \tilde{u}_2^T(N-1)]^T$ where $\tilde{u}_2(k) = [\tilde{u}_{2,1}(k), \dots, \tilde{u}_{2,p}(k)]^T \in \mathbb{R}^p$.

Now consider the minimum-phase, discrete-time, LTI, MIMO system:

$$\begin{aligned} \tilde{x}(k+1) &= A_{\mathcal{L}_1} \tilde{x}(k) + B_{\mathcal{L}_1} \tilde{u}_2(k) \\ \tilde{y}_2(k) &= C_{\mathcal{L}_1} \tilde{x}(k), \end{aligned} \quad (10)$$

where $A_{\mathcal{L}_1}$, $B_{\mathcal{L}_1}$ and $C_{\mathcal{L}_1}$ are the discrete-time matrices that describe system (9). Using the lifted representation, we can write the system (10) as:

$$\tilde{y}_{2,j} = \tilde{\mathbf{F}}_{\text{ILC}} \tilde{u}_{2,j} + \tilde{\mathbf{d}}_{\infty} \quad (11)$$

where the subscript j represents the iteration number, $\tilde{\mathbf{F}}_{\text{ILC}}$ is a constant matrix derived from the discretized model (10) as described in [21] and $\tilde{\mathbf{d}}_{\infty}$ represents a repetitive disturbance that is initially unknown, but is identified during the learning process. In many control applications, constraints must be placed on the process variables to ensure safe and smooth operations. The system may be subjected to input or output constraints of the form:

$$S_c \tilde{y}_2 \leq \tilde{y}_{2,max}, \quad Z_c \tilde{u}_2 \leq \tilde{u}_{2,max}, \quad (12)$$

where S_c and Z_c are matrices of appropriate size.

An iteration-domain Kalman filter is used to obtain an estimate of the disturbance $\hat{\mathbf{d}}_{j|j}$, based on measurements from iterations $1, \dots, j$ (see [21] and [14] for further details). Using (11) and the estimated disturbance, the estimated output error $\hat{\mathbf{y}}_{2,j+1|j}$ can be represented by:

$$\hat{\mathbf{y}}_{2,j+1|j} = \tilde{\mathbf{F}}_{\text{ILC}} \tilde{u}_{2,j+1} + \hat{\mathbf{d}}_{j|j}. \quad (13)$$

At the end of iteration j an update step computes the next input sequence $\tilde{\mathbf{u}}_{2,j+1}$ that minimizes the estimated output error $\hat{\mathbf{y}}_{2,j+1|j}$ and the control effort $\tilde{\mathbf{u}}_{2,j+1}$ based on the following cost function:

$$J(\tilde{\mathbf{u}}_{2,j+1}) = \hat{\mathbf{y}}_{2,j+1|j} \mathbf{Q} \hat{\mathbf{y}}_{2,j+1|j} + \tilde{\mathbf{u}}_{2,j+1} \mathbf{R} \tilde{\mathbf{u}}_{2,j+1},$$

subject to (12), where \mathbf{Q} is a constant, positive semidefinite matrix and \mathbf{R} is a constant, positive definite matrix. The resulting convex optimization problem can be solved efficiently with state-of-the-art optimization libraries. In this work, we use IBM ILOG CPLEX Optimizer [22].

Remark 3. *If the source and target systems have underlying \mathcal{L}_1 adaptive controllers with different reference models, then it is still possible to implement the multi-robot framework by using the reference models to build a map from the source system to the target system [6]. Using this map, trajectories learned on the source system can be transferred to the target system, which has a different reference model.*

B. Multi-task transfer

Our proposed multi-task transfer learning framework uses insights from control systems theory and knowledge of a single previously learned trajectory to calculate the reference input of a new, unseen trajectory to minimize the trajectory tracking error. As shown in Section IV-A, the input-output behavior of the system under extended \mathcal{L}_1 adaptive control is LTI, MIMO and minimum-phase, see (9). We use (1) to describe the controlled system and assume it is minimum-phase.

Lemma 1. *Consider a minimum-phase, discrete-time, MIMO, LTI system (1), and a smooth desired trajectory \mathbf{y}_2^* . Then, there exists a control input sequence \mathbf{u}_2 that achieves perfect tracking of \mathbf{y}_2^* . Moreover, at time instant k , the control input $u_2(k)$ can be represented as a linear combination of the state $x(k)$ and the values $y_{2,1}^*(k+r_1), \dots, y_{2,p}^*(k+r_p)$, where $y_{2,i}^*(j)$ is the value of the i^{th} component of the desired output at time index j , and (r_1, \dots, r_p) is the vector relative degree of the system.*

Proof. From Definition 1 the matrix A_0 is nonsingular. Hence, we can define the following control law:

$$\begin{bmatrix} u_{2,1}(k) \\ \vdots \\ u_{2,p}(k) \end{bmatrix} = A_0^{-1} \left(\begin{bmatrix} -C_1 A^{r_1} \\ \vdots \\ -C_p A^{r_p} \end{bmatrix} x(k) + \begin{bmatrix} y_{2,1}^*(k+r_1) \\ \vdots \\ y_{2,p}^*(k+r_p) \end{bmatrix} \right). \quad (14)$$

By assumption, the desired trajectory $y_2^*(k)$, $k \geq 0$, is known. Hence, at time step k , $y_{2,1}^*(k+r_1), \dots, y_{2,p}^*(k+r_p)$ are all known, and (14) can be realized.

Next, by plugging the control law (14) into (2), we obtain:

$$\begin{bmatrix} y_1(k+r_1) \\ \vdots \\ y_p(k+r_p) \end{bmatrix} = \begin{bmatrix} y_{2,1}^*(k+r_1) \\ \vdots \\ y_{2,p}^*(k+r_p) \end{bmatrix}. \quad (15)$$

Since the system (1) is minimum-phase by assumption, then as discussed in Section II, the control input $u_2(k) = -A_0^{-1}[(C_1 A^{r_1})^T, \dots, (C_p A^{r_p})^T]^T x(k)$ achieves asymptotic stability of the internal dynamics of (1). Since for linear systems asymptotic stability implies bounded-input, bounded-output (BIBO) stability, then it is evident that under the control law (14) and for bounded reference input y_2^* , the internal states of (1) are bounded.

Finally, by applying the control law (14) at each time step k , $k \geq 0$, we have from (15), $y_i(\tilde{k}) = y_{2,i}^*(\tilde{k})$, for each $\tilde{k} \geq r_i$, i.e., the perfect tracking condition is achieved. From the control law (14), the input $u_2(k)$ is a linear combination of $x(k)$ and $y_{2,1}^*(k+r_1), \dots, y_{2,p}^*(k+r_p)$, which completes the proof. \square

Suppose that we are given a smooth desired trajectory \mathbf{y}_2^* and using a learning approach, such as ILC, we are able to compute for this particular desired trajectory an input sequence vector \mathbf{u}_2 that achieves perfect tracking performance. Similar to [8], we use the desired output and learned input trajectories $(\mathbf{y}_2^*, \mathbf{u}_2)$ to learn a transfer learning map \mathcal{M} that minimizes the transfer learning error as in (3). Unlike [8], in which the map is constructed through experimental trial-and-error, we use Lemma 1 to construct the map. In particular, we know from Lemma 1 that to achieve perfect tracking, $u_{2,i}(k)$, $i = 1, \dots, p$, should be a linear combination of $x(k)$ and $y_{2,1}^*(k+r_1), \dots, y_{2,p}^*(k+r_p)$, where (r_1, \dots, r_p) is the vector relative degree of (1). We assume, for now, that the state $x(k)$ can be measured or estimated and stored. Hence, we propose to build, with the available information, the following windowing function:

$$W(\mathbf{x}, \mathbf{y}_2^*) = \begin{bmatrix} x^T(0) & \bar{y}_{2,i}^*(0) \\ \vdots & \vdots \\ x^T(N_r) & \bar{y}_{2,i}^*(N_r) \end{bmatrix}, \quad (16)$$

where $\bar{y}_{2,i}^*(a) = [y_{2,1}^*(a+r_1), \dots, y_{2,p}^*(a+r_p)]$, and $N_r = N - \max_{j \in \{1, \dots, p\}}(r_j)$. Using the windowing function $W(\mathbf{x}, \mathbf{y}_2^*)$, we define the following learning process

$$\mathbf{u}_{2,i} = W(\mathbf{x}, \mathbf{y}_2^*) \theta_i, \quad (17)$$

where $\mathbf{u}_{2,i} = [u_{2,i}(0), \dots, u_{2,i}(N_r)]^T$ is the collection of the i^{th} elements of \mathbf{u}_2 , determined from the ILC algorithm. This is a least-squares problem for the parameter vector $\theta_i \in \mathbb{R}^{n+p}$.

Remark 4. *The vectors of unknowns θ_i , $i \in \{1, \dots, p\}$, are all functions of the system matrices A , B , C , which is evident from (14) and the definition of the matrix A_0 in Definition 1. We emphasize that the vectors θ_i do not depend on the desired trajectory \mathbf{y}_2^* or the system states.*

Therefore, we can reuse the calculated vectors θ_i , that build an invariant map, to calculate for new, unseen, desired trajectories correct input vectors that achieve perfect tracking. In particular, we use the vectors θ_i to calculate the control input that achieves perfect tracking of a new desired

trajectory $\mathbf{y}_2^{*,new}$ as follows:

$$u_{2,i}^{new}(k) = \left[x^T(k) \quad \bar{y}_{2,i}^{*,new}(k) \right] \theta_i \quad \forall i \in \{1, \dots, p\}, \quad (18)$$

where θ_i , $i \in \{1, \dots, p\}$ are calculated by (17) and $\bar{y}_{2,i}^{*,new}(k) = [y_{2,1}^{*,new}(k+r_1), \dots, y_{2,p}^{*,new}(k+r_p)]$.

Remark 5. Our proposed control law (18) is obtained from input-output data and does not assume the knowledge of the system matrices A , B and C as in (14). It only assumes the knowledge of the vector relative degree of the system, which can be calculated from (9), or obtained through experiments, see Remark 2.

Notice that the construction of the windowing function $W(\mathbf{x}, \mathbf{y}_2^*)$ requires the knowledge of the system states or estimated values of the states using an estimator, for example, a Kalman filter. We now discuss how the proposed transfer learning approach can be extended to the case where the state measurements or their estimated values are not available. To this end, we review an important Lemma from [23].

Lemma 2. Consider the discrete-time, LTI system (1), and suppose that the pair (A, C) is observable. Then, the system state $x(k)$ is given uniquely in terms of input-output sequences as follows:

$$x(k) = M_u \begin{bmatrix} u(k-1) \\ \vdots \\ u(k-\bar{N}) \end{bmatrix} + M_y \begin{bmatrix} y(k-1) \\ \vdots \\ y(k-\bar{N}) \end{bmatrix}, \quad (19)$$

where \bar{N} is an upper bound on the system's observability index, $M_u = U_{\bar{N}} - M_y T_{\bar{N}}$, $M_y = A^{\bar{N}} V_{\bar{N}}^+$, $V_{\bar{N}}^+ = (V_{\bar{N}}^T V_{\bar{N}})^{-1} V_{\bar{N}}^T$ is the left inverse of the observability matrix $V_{\bar{N}}$, and

$$U_{\bar{N}} = \begin{bmatrix} B & AB & \dots & A^{\bar{N}-1}B \end{bmatrix},$$

$$T_{\bar{N}} = \begin{bmatrix} 0 & CB & CAB & \dots & CA^{\bar{N}-2}B \\ 0 & 0 & CB & \dots & CA^{\bar{N}-3}B \\ \vdots & \vdots & \ddots & \ddots & \vdots \\ 0 & \dots & 0 & CB \\ 0 & 0 & 0 & 0 & 0 \end{bmatrix},$$

$$V_{\bar{N}} = \begin{bmatrix} (CA^{\bar{N}-1})^T & \dots & (CA)^T & C^T \end{bmatrix}^T.$$

In other words, if the system (1) is observable, then the state vector can be represented as a linear combination of a finite sequence of past inputs and outputs of the system. From Lemmas 1 and 2, it can be shown that the control input $u_2(k)$ that achieves perfect tracking of the desired trajectory can be represented as a linear combination of $u_2(k-1), \dots, u_2(k-\bar{N}), y(k-1), \dots, y(k-\bar{N}), y_{2,1}^*(k+r_1), \dots, y_{r,p}^*(k+r_p)$, where $y(k)$ is the actual output of the system, (r_1, \dots, r_p)

is the vector relative degree of (1) and \bar{N} is an upper bound of the observability index of (1).

Hence, for observable systems, our approach is still valid when only input-output data is available. In this case, the ILC algorithm will also be used to calculate an input \mathbf{u} that will make the output \mathbf{y} perfectly track the desired trajectory \mathbf{y}_2^* . Using this input-output information, we can redefine the windowing function (16) by substituting the state $x(k)$ with a finite sequence of input-output information such that:

$$W_{IO}(\mathbf{u}, \mathbf{y}, \mathbf{y}_2^*) = \begin{bmatrix} \bar{u}(\bar{N}) & \bar{y}(\bar{N}) & \bar{y}_{2,i}^*(\bar{N}) \\ \vdots & \vdots & \vdots \\ \bar{u}(N_r) & \bar{y}(N_r) & \bar{y}_{2,i}^*(N_r) \end{bmatrix}, \quad (20)$$

where $\bar{y}_{2,i}^*(a) = [y_{2,1}^*(a+r_1), \dots, y_{2,p}^*(a+r_p)]$, $\bar{u}(a) = [u^T(a-1), \dots, u^T(a-\bar{N})]$, and $\bar{y}(a) = [y^T(a-1), \dots, y^T(a-\bar{N})]$. Similar to (17), we then calculate the vectors of unknown parameters $\theta_{IO,i}$. The vectors are functions of the matrices of system (1) and can be used to calculate the required input when a new, unseen trajectory is encountered. For this case, the proposed control law is:

$$u_{2,i}^{new}(k) = \left[\bar{u}(k) \quad \bar{y}(k) \quad \bar{y}_{2,i}^{*,new}(k) \right] \theta_{IO,i}, \quad \forall i \in \{1, \dots, p\}.$$

In order to allow the system to continue learning after transfer, we need to provide the ILC with an initial estimation of the repetitive disturbance $\hat{\mathbf{d}}_{0,trans}$. We assume that the calculated input \mathbf{u}_2^{new} achieves perfect tracking of the new trajectory; hence, $\hat{\mathbf{y}}_{2,j+1|j}$ in (13) is 0. Using (13) and the calculated input \mathbf{u}_2^{new} , we are able to calculate the disturbance $\hat{\mathbf{d}}_{0,trans}$.

In this subsection, we derived the multi-task transfer learning framework for linear/linearized systems, which is not a big loss of generality given that the underlying \mathcal{L}_1 adaptive controller makes the considered closed-loop system approximately behave as a linear model. Nevertheless, it should be noted that the proposed framework can be also extended to **nonlinear systems** with well-defined vector relative degrees and stable inverse dynamics. In particular, analogous to Lemma 1, it can be shown that there exists a control input satisfying perfect tracking of an arbitrary, smooth trajectory \mathbf{y}_2^* , and this input is a nonlinear function of the state $x(k)$ and the values $y_{2,1}^*(k+r_1), \dots, y_{2,p}^*(k+r_p)$, where (r_1, \dots, r_p) is the system's vector relative degree. In practice, one can use a nonlinear regression model, e.g., a neural network or a Gaussian Process, to approximate this unknown nonlinear function [9], [10]. Alternatively, smooth nonlinear systems can be approximated by piecewise affine/linear systems with arbitrary accuracy [24]. One can construct a cover/partition of the state space of a nonlinear system, and represent the nonlinear system in each region of the cover with a local, affine/linear model. One can use the above proposed results to define a linear transfer learning map for each local region, resulting overall in a piecewise linear transfer learning map. The details will be further studied in future publications.



Fig. 3. The two different quadrotors used in the experiments. The quadrotor on the left is the Bebop 2, and on the right is the AR.Drone 2.0.

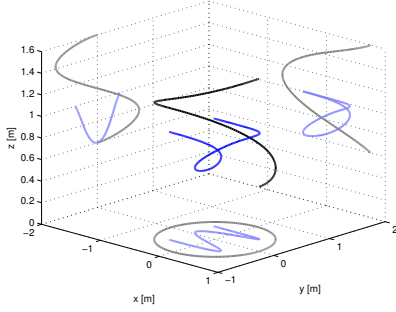


Fig. 4. Two different trajectories are used to test the multi-task framework. The source trajectory is depicted in black and the target trajectory is depicted in blue. Projections of both trajectories in the $x-y$, $x-z$ and $y-z$ planes in light blue and gray are also shown.

V. EXPERIMENTAL RESULTS

This section shows the experimental results of the proposed multi-robot, multi-task framework applied to quadrotors for high-accuracy trajectory tracking. We focus on two different scenarios: (i) multi-robot, multi-task transfer learning, and (ii) multi-task transfer learning. The reader is referred to [14] for experimental results of the multi-robot transfer learning framework.

The vehicles used in the experiments are the Parrot AR.Drone 2.0 and the Parrot Bebop 2 (see Fig. 3). Each quadrotor has an underlying \mathcal{L}_1 adaptive controller that makes both behave close to the reference system. In what follows, the signals $u_{1,x}(t)$, $u_{1,y}(t)$, $u_{1,z}(t)$, $u_{2,x}(t)$, $u_{2,y}(t)$, $u_{2,z}(t)$, $y_{1,x}(t)$, $y_{1,y}(t)$, $y_{1,z}(t)$ and $y_{2,x}(t)$, $y_{2,y}(t)$, $y_{2,z}(t)$ are the desired translational velocity, desired position, quadrotor translational velocity and quadrotor position each in the x, y, z directions, respectively. A central overhead motion capture camera system provides position, roll-pitch-yaw Euler angles and rotational velocity measurements and through numerical differentiation, we obtain velocities. To quantify the tracking performance, an average position error along the trajectory is defined by:

$$e = \frac{\sum_{i=1}^N \sqrt{e_x^2(i) + e_y^2(i) + e_z^2(i)}}{N}, \quad (21)$$

where $e_x(i) = u_{2,x}(i) - y_{2,x}(i)$, $e_y(i) = u_{2,y}(i) - y_{2,y}(i)$ and $e_z(i) = u_{2,z}(i) - y_{2,z}(i)$. We propose two different trajectories to test our approach, as shown in Fig. 4, a source (black) and a target (blue) trajectory.

A. Multi-robot, multi-task transfer learning

To test the multi-robot, multi-task transfer learning framework, we first use the multi-robot framework presented in Section IV-A to train the Bebop 2, for ten iterations, to

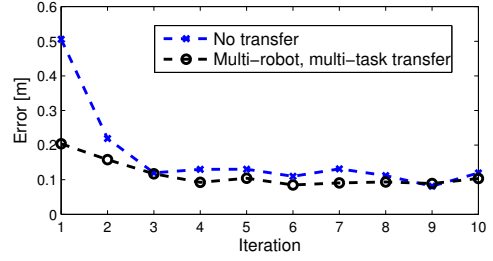


Fig. 5. Average position error over ILC iterations of the AR.Drone 2.0 tracking the target trajectory when (i) information from the Bebop 2 tracking the source trajectory and the proposed multi-robot, multi-task framework are used to calculate the reference signal of the first iteration (depicted in black), and (ii) no transfer information is used to calculate the reference signal of the first iteration (depicted in blue).

accurately track the source trajectory in Fig. 4. Next, using the multi-task framework described in Section IV-B, we generalize this trajectory to the target trajectory to be applied to the AR.Drone 2.0. Fig 5 shows the average position errors of the AR.Drone 2.0 tracking the target trajectory when the multi-robot, multi-task framework is used, and when no transfer learning information is used. The proposed multi-robot, multi-task transfer framework reduces the tracking error by almost 60% in the first iteration. This is important as high initial errors can cause risks, e.g., collisions.

B. Multi-task transfer learning

Next, we test the multi-task (MT) transfer learning framework. As discussed in the previous subsection, we first use the combined \mathcal{L}_1 adaptive controller and ILC framework to train the Bebop 2, for ten iterations, to accurately track the source trajectory. Then, using the multi-task framework described in Section IV-B, we generalize this trajectory to a target trajectory to be applied on the Bebop 2. Fig. 6 shows the target trajectory in the x -axis on the left, y -axis in the center and z -axis on the right. For each axis, the output trajectories followed at iterations 1 and 10 when the MT transfer framework is used are shown together with the output trajectory followed at iteration 1 when no transfer is used. It is clear that the MT framework significantly reduces the tracking error in the first iteration. Moreover, Fig. 7 shows the average position errors of the Bebop 2 tracking the target trajectory when the multi-task framework is used, as described above, and when no transfer learning information is used. The multi-task transfer framework reduces the tracking error by almost 75% in the first iteration.

VI. CONCLUSIONS

In this paper, we introduced a multi-robot, multi-task transfer learning framework for MIMO systems that allows a target system to accurately complete a target task using few demonstrations of a source task on a source system. We focused on the trajectory tracking problem as many robotic tasks can be transformed into such a problem. The multi-robot transfer learning framework is based on a combined \mathcal{L}_1 adaptive controller and ILC. The key concept is that the \mathcal{L}_1 adaptive controller forces systems to behave like a specified linear reference model. Hence, learned tasks on a source

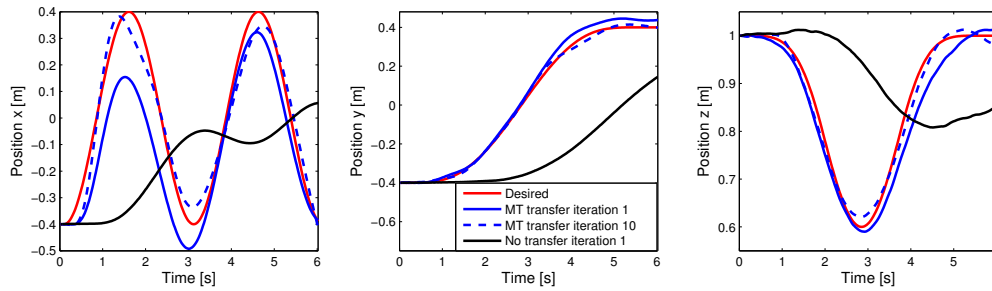


Fig. 6. The target trajectory followed by the Bebop 2 in each axis (i) at iteration 1 (solid blue line) and (ii) at iteration 10 (dashed blue line), when information from the Bebop 2 tracking the source trajectory and the proposed multi-task framework are used to calculate the reference signal of the first iteration, and (iii) at iteration 10 (solid black line) when no transfer information is used to calculate the reference signal of first iteration.

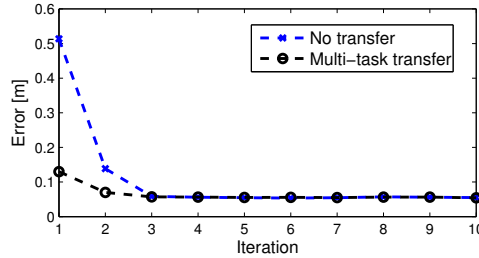


Fig. 7. Average position error over ILC learning iterations of the Bebop 2 tracking the target trajectory when (i) information from the Bebop 2 tracking the source trajectory and the proposed multi-task framework are used to calculate the reference signal of the first iteration (depicted in black), and (ii) no transfer information is used to calculate the reference signal of first iteration (depicted in blue).

system can be directly transferred to target systems. The multi-task transfer learning framework uses control theory results to build a time- and state-invariant map from the desired trajectory to the correct input that accurately tracks that trajectory. Since this map is proved to be time- and state-invariant, it can be used to generate new correct inputs for new, unseen desired trajectories. Experimental results on two different quadrotor platforms show that the proposed multi-robot, multi-task transfer learning framework is able to use a single source trajectory learned on the source system to significantly decrease the tracking error of a target trajectory on a target system.

REFERENCES

- [1] R. Skelton, "Model error concepts in control design," *International Journal of Control*, vol. 49, no. 5, pp. 1725–1753, 1989.
- [2] M. Morari and J. H. Lee, "Model predictive control: past, present and future," *Computers & Chemical Engineering*, vol. 23, no. 4, pp. 667–682, 1999.
- [3] S. Skogestad and I. Postlethwaite, *Multivariable feedback control: analysis and design*. Wiley New York, 2007, vol. 2.
- [4] K. V. Raimalwala, B. A. Francis, and A. P. Schoellig, "An upper bound on the error of alignment-based transfer learning between two linear, time-invariant, scalar systems," in *Proc. of the IEEE/RSJ International Conference on Intelligent Robots and Systems (IROS)*, 2015, pp. 5253–5258.
- [5] —, "A preliminary study of transfer learning between unicycle robots," in *AAAI Spring Symposium Series*, 2016.
- [6] M. K. Helwa and A. P. Schoellig, "Multi-robot transfer learning: A dynamical system perspective," *arXiv preprint arXiv:1707.08689*, Accepted at IROS 2017.
- [7] B. Bocsi, L. Csató, and J. Peters, "Alignment-based transfer learning for robot models," in *Proc. of the International Joint Conference on Neural Networks (IJCNN)*. IEEE, 2013, pp. 1–7.
- [8] M. Hamer, M. Waibel, and R. D'Andrea, "Knowledge transfer for high-performance quadcopter maneuvers," in *Proc. of the IEEE/RSJ International Conference on Intelligent Robots and Systems (IROS)*, 2013, pp. 1714–1719.
- [9] S. Zhou, M. K. Helwa, and A. P. Schoellig, "Design of deep neural networks as add-on blocks for improving impromptu trajectory tracking," *arXiv preprint arXiv:1705.10932*, Accepted at CDC 2017.
- [10] Q. Li, J. Qian, Z. Zhu, X. Bao, M. K. Helwa, and A. P. Schoellig, "Deep neural networks for improved, impromptu trajectory tracking of quadrotors," in *Proc. of the IEEE International Conference on Robotics and Automation (ICRA)*, 2017, pp. 5183–5189.
- [11] D. J. Hoelzle, A. G. Alleyne, and A. J. W. Johnson, "Bumpless transfer for a flexible adaptation of iterative learning control," in *Proc. of the American Control Conference (ACC)*, 2011, pp. 4305–4311.
- [12] Y. Duan, M. Andrychowicz, B. Stadie, J. Ho, J. Schneider, I. Sutskever, P. Abbeel, and W. Zaremba, "One-shot imitation learning," *arXiv preprint arXiv:1703.07326*, 2017.
- [13] C. Devin, A. Gupta, T. Darrell, P. Abbeel, and S. Levine, "Learning modular neural network policies for multi-task and multi-robot transfer," in *Proc. of the IEEE International Conference on Robotics and Automation (ICRA)*, 2017, pp. 2169–2176.
- [14] K. Pereida, R. R. Duijvenvoorden, and A. P. Schoellig, "High-precision trajectory tracking in changing environments through \mathcal{L}_1 adaptive feedback and iterative learning," in *Proc. of the IEEE International Conference on Robotics and Automation (ICRA)*, 2017, pp. 344–350.
- [15] A. Isidori, *Nonlinear Control Systems*. Springer-Verlag London Limited, 1995.
- [16] M. A. Henson and D. E. Seborg, "Feedback linearizing control," *Nonlinear process control*, pp. 149–231, 1997.
- [17] H. Jafamejadsani, H. Lee, N. Hovakimyan, and P. Voulgaris, "A multirate adaptive control for mimo systems with application to cyber-physical security," in *Proc. of the IEEE Conference on Decision and Control (CDC)*, 2017 [Submitted].
- [18] H. Lee, " \mathcal{L}_1 adaptive control for nonlinear and non-square multivariable systems," Ph.D. dissertation, University of Illinois at Urbana-Champaign, 2017 [Submitted to IEEE TAC].
- [19] N. Hovakimyan and C. Cao, *\mathcal{L}_1 Adaptive Control Theory: Guaranteed Robustness with Fast Adaptation*. Philadelphia, PA: Society for Industrial and Applied Mathematics, 2010.
- [20] A. P. Schoellig and R. D'Andrea, "Optimization-based iterative learning control for trajectory tracking," in *Proc. of the European Control Conference (ECC)*, 2009, pp. 1505–1510.
- [21] A. P. Schoellig, F. L. Mueller, and R. D'Andrea, "Optimization-based iterative learning for precise quadcopter trajectory tracking," *Autonomous Robots*, vol. 33, no. 1-2, pp. 103–127, 2012.
- [22] IBM ILOG CPLEX Optimizer, Last accessed 08 Sep 2017. [Online], available: <http://www-01.ibm.com/software/commerce/optimization/cplex-optimizer/index.html>.
- [23] F. L. Lewis and K. G. Vamvoudakis, "Reinforcement learning for partially observable dynamic processes: adaptive dynamic programming using measured output data," *IEEE Transactions on Systems, Man, and Cybernetics, Part B (Cybernetics)*, vol. 41, no. 1, pp. 14–25, 2011.
- [24] M. K. Helwa and P. E. Caines, "Epsilon controllability of nonlinear systems on polytopes," in *Proc. of the IEEE Conference on Decision and Control (CDC)*, 2015, pp. 252–257.